



### Science Arts & Métiers (SAM)

is an open access repository that collects the work of Arts et Métiers Institute of Technology researchers and makes it freely available over the web where possible.

This is an author-deposited version published in: <https://sam.ensam.eu>  
Handle ID: <http://hdl.handle.net/10985/11878>

#### To cite this version :

Lamice DENGUIR, Jose Carlos MARTINS DO OUTEIRO, Joël RECH, Guillaume FROMENTIN, Vincent VIGNAL, Rémy BESNARD - Friction Model for Tool/Work Material Contact Applied to Surface Integrity Prediction in Orthogonal Cutting Simulation - In: 16th CIRP CMMO, France, 2017-06-16 - Procedia CIRP - 2017

Any correspondence concerning this service should be sent to the repository

Administrator : [scienceouverte@ensam.eu](mailto:scienceouverte@ensam.eu)



16<sup>th</sup> CIRP Conference on Modelling of Machining Operations

## Friction model for tool/work material contact applied to surface integrity prediction in orthogonal cutting simulation

L. A. Denguir<sup>a,c,\*</sup>, J. C. Outeiro<sup>a</sup>, J. Rech<sup>b</sup>, G. Fromentin<sup>a</sup>, V. Vignal<sup>c,e</sup>, R. Besnard<sup>d,e</sup>

<sup>a</sup>LaBoMaP-Arts et Metiers ParisTech, rue Porte de Paris, Cluny 71250, FRANCE

<sup>b</sup>LTDS, UMR CNRS 5513, Ecole Nationale d'Ingénieurs de Saint Etienne rue Jean Parot, Saint-Etienne 42023, FRANCE

<sup>c</sup>ICB UMR CNRS 6303, Université de Bourgogne-Franche Comté, BP 47870, 21078 Dijon, FRANCE

<sup>d</sup>CEA Valduc, 21120 Is sur Tille, FRANCE

<sup>e</sup>LIMPE (Interaction Matériau-Procédé-Environnement), LRC DAM-VA-11-02, Dijon, FRANCE

\* Corresponding author. Tel.: +33-3-85-59-53-88; fax: +33-3-85-59-53-70. E-mail address: [Lamice.DENGUIR@ensam.eu](mailto:Lamice.DENGUIR@ensam.eu)

### Abstract

Tribological behavior at both tool/chip and tool/work material interfaces should be highly considered while simulating the machining process. In fact, it is no longer accurate to suppose one independent constant friction coefficient at the tool/chip interface, since in reality it depends on the applied contact conditions, including the sliding velocity and pressure. The contact conditions at both above mentioned interfaces may affect the thermal and mechanical phenomena and consequently the surface integrity predictions.

In this article, the influence of contact conditions (sliding velocity) on the tribological behavior of uncoated tungsten carbide tool against OFHC copper work material was investigated. Series of tribology tests combined with numerical simulations of the contact process were performed under different sliding speeds and contact pressures, in order to identify the friction coefficient and the heat partition between OFHC copper and tungsten carbide. The friction coefficient in function of the sliding velocity was then integrated into a FE model of the orthogonal cutting of OFHC copper and applied to surface integrity prediction.

© 2017 The Authors. Published by Elsevier B.V. This is an open access article under the CC BY-NC-ND license

(<http://creativecommons.org/licenses/by-nc-nd/4.0/>).

Peer-review under responsibility of the scientific committee of The 16th CIRP Conference on Modelling of Machining Operations

**Keywords:** friction modeling; tribology tests; cutting simulation; carbide tool; OFHC copper.

### 1. Introduction

Productivity improvement of machining operations requires the optimization of tool geometry and cutting conditions. In parallel, a special attention should be paid to the surface integrity of machined parts, since the cutting conditions have an influence on the functional performance and life of such parts [1]. Modelling and simulation of metal cutting is a way to enable this optimization and to ensure the quality of machined surfaces. Among the key input data necessary for metal cutting models, a friction model between the work material and the cutting tool is required. However, obtaining realistic friction data for metal cutting simulation of Oxygen Free High Conductivity (OFHC) copper remains an issue for several reasons. First, its mechanical [2] and

tribological behaviors depend on the heat treatment applied to this material. Second, the cutting under dry, near dry or with incorrect lubricant can generate work material adhesion to the tool, affecting dramatically the friction coefficient [3].

Most of the literature dealing with metal cutting modelling considers a constant Coulomb friction coefficient [5, 6, 7], which does not corresponds to the reality. The values of the friction coefficient reported in the literature for OFHC copper vary between 0.1 [5] and 0.7 [10] depending on several factors, including: tool material, tool surface roughness, lubrication conditions, sliding speed and contact pressure. Finally, Astakhov has shown that the presence of a cutting fluid can reduce dramatically the friction coefficient during machining, and its effect depends on the nature of the fluid [3].

The conditions used to determine the friction coefficient are rarely reported in the literature, which makes it difficult to be used in further investigations.

The current study proposes a friction model for the contact between the OFHC copper and the uncoated cemented tungsten carbide cutting tool, under forced cooled air conditions. This friction model considers the friction coefficient as a function of the sliding velocity only.

## 2. Determination of the friction coefficient

After characterizing the tribology ruling the tool/material contact while the cutting operation, a contact law is here proposed. To identify the coefficients relative to this law, friction tests are performed.

### 2.1. Mechanical and thermo-physical properties of the tool and work materials

The cutting tool is made of uncoated cemented tungsten carbide (grade ISO M10, ANSI C7). The work material is Oxygen Free High Conductivity (OFHC) copper annealed at 450°C for 2 hours. The thermo-mechanical properties of the interacting tool/work material are given in Table 1 [11, 13].

Table 1. The tool and work material properties.

Properties	Unit	Value for carbide	Value for copper
Density	kg/m <sup>3</sup>	14450	8960
Young modulus E	GPa	630	127
Poisson coefficient $\nu$		0.3	0.33
Conductivity $\kappa$	W/mK	44.6	401
Specific heat $C_p$	J/kgK	226	380
Expansion $\alpha$	°K <sup>-1</sup>	----	1.4E-5

### 2.2. Tribological tests: theory

The test aims to measure the apparent macroscopic friction coefficient,  $\mu_{app}$ , corresponding to the ratio  $F_t/F_n$ , where  $F_n$  is the normal force and  $F_t$  is the tangential force, which were applied on the pin. The apparent friction coefficient may be decomposed into an elasto-plastic deformation coefficient,  $\mu_{def}$ , and an interfacial friction coefficient,  $\mu_{adh}$ , also called adhesive friction coefficient as follows:

$$\mu_{app} = \frac{F_t}{F_n} = \mu_{adh} + \mu_{def} \quad (1)$$

The friction test results are treated to separate the adhesive friction coefficient from the apparent one. This treatment is performed after analyzing the work material deposits on the pin head. Analysis is done by applying Eq. 2 to Eq. 9. The geometrical parameters used in those equations are represented in Fig. 1.

$$\vec{F}_n = (BP - D\tau) \cdot \vec{Z} \quad (2)$$

$$\vec{F}_t = (AP + C\tau) \cdot \vec{X} \quad (3)$$

$$A = D = \left| \int_{S_c} (dS \vec{n} \cdot \vec{X}) \right| = \left| \int_{S_c} (dS \vec{t} \cdot \vec{Z}) \right| \quad (4)$$

$$B = C = \left| \int_{S_c} (dS \vec{n} \cdot \vec{Z}) \right| = \left| \int_{S_c} (dS \vec{t} \cdot \vec{X}) \right| \quad (5)$$

$$S_r = (R^2 - a^2 \sin^2 \omega) \sin^{-1}(a \cos \omega / r) - a \cos \omega \sqrt{R^2 - a^2} \quad (6)$$

$$r = \sqrt{R^2 - a^2 \sin^2 \omega} \quad (7)$$

$$\mu_{app} = \frac{\left| \frac{\vec{F}_t}{F_n} \right|}{\left| \frac{\vec{F}_n}{F_n} \right|} = \frac{AP + C\tau}{BP - D\tau} = \frac{AP + C\mu_{adh}}{BP - D\mu_{adh}} \quad (8)$$

$$\mu_{adh} = \frac{B\mu_{app} - A}{C + D\mu_{app}} \quad (9)$$

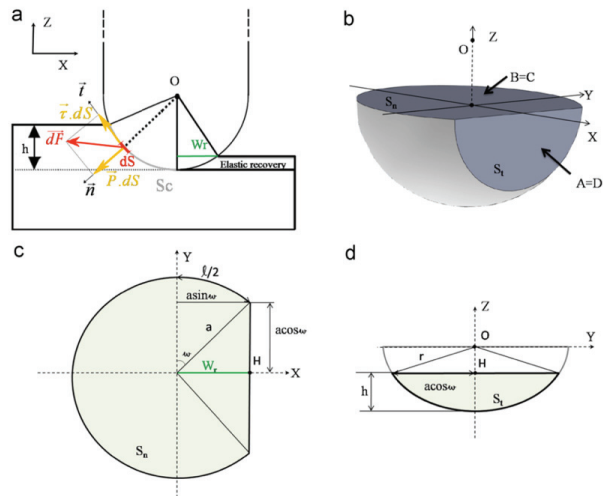


Fig. 1. Geometry of the surface/pin contact in a friction test: (a) friction of the pin on the surface; (b) perspective view of the portion of the pin head engaged in the work material; (c) geometry of the rubbed material print on the pin head in an XY plan and (d) in a ZY plan [4].

### 2.3. Tribological tests: experimental setup

Tribological tests aim to identify a friction model able to describe the interaction between the carbide tool and the OFHC copper in the presence of forced cooled air supplied by a Vortex system (-5 ± 2 °C, 6 bar).

The experimental setup (Fig. 2) is composed by a cylindrical bar of Ø85 mm diameter in OFHC copper mounted on a CNC lathe machine, animated with a rotation speed, and a pin of uncoated tungsten carbide with a spherical head diameter of Ø34 mm is rubbing over the cylindrical surface of the bar. The pin is moving along the bar axis direction with a constant feed of 0.18 mm/rev. Simultaneously, normal force ( $F_n$ ) to the bar surface is applied by the pin through a hydraulic actuator. A piezoelectric dynamometer is used to measure this force, as well as the tangential force, and a thermocouple is placed on the pin to

measure its temperature. The same Vortex cooling system as the one used in metal cutting tests is used in these tribological tests.

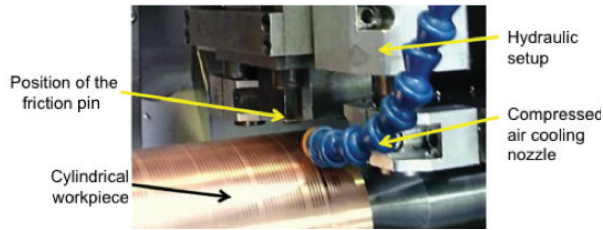


Fig. 2. Setup of the tribological test.

The tests were performed using 5 sliding velocities (10; 20; 40; 80 and 120 m/min) and two normal forces (200 N and 500 N). Every test condition is repeated twice.

After performing these tests, the contact radius,  $a$ , and the rear distance,  $W$  (see Fig. 3), were measured over the pins, using an optical microscopy. Then, the adhesive friction coefficient is calculated as explained in the previous section.

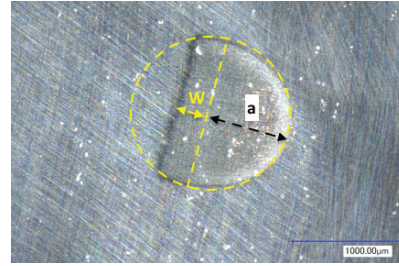


Fig. 3. Example of contact zones on pins (pin diameter of 34 mm, pressing force of 500 N and sliding velocity of 40 m/min).

#### 2.4. Tribological tests: experimental results

The tribological tests results are presented in Table. 2.

Table 2. Friction tests results.

Sliding velocity (m/min)	Normal force (N)	Friction force (N)	Apparent friction coefficient $\mu_{app}$	Sliding distance (m)	Contact radius, $a$ (mm)	Rear distance, $W$ (mm)	Adhesive friction Coefficient, $\mu_{adh}$
10	204	33	0.16	1.54	0.62	0.12	0.04
10	204	35	0.17	1.54	0.39	0.12	0.12
10	506	116	0.23	1.49	0.62	0.20	0.16
10	505	116	0.23	1.49	0.57	0.24	0.19
20	212	45	0.21	3.84	0.53	0.20	0.16
20	203	41	0.20	3.81	0.65	-0.10	0.37
20	495	124	0.25	3.74	0.57	0.36	0.23
20	479	110	0.23	3.63	0.64	0.12	0.10
40	219	44	0.20	7.63	0.63	-0.05	0.52
40	207	79	0.38	7.57	0.47	0.12	0.31
40	498	229	0.46	7.42	0.66	0.25	0.39
40	517	129	0.25	7.37	0.64	0.17	0.16
80	217	43	0.20	15.04	0.49	0.10	0.11
80	223	42	0.19	15.04	0.50	0.20	0.15
80	498	110	0.22	14.63	0.63	0.17	0.13
80	519	130	0.25	14.63	0.65	0.22	0.18
120	232	72	0.31	22.72	0.72	0.22	0.22
120	221	42	0.19	22.57	0.61	0.13	0.08
120	512	123	0.24	22.10	0.65	0.19	0.16
120	529	85	0.16	21.94	0.71	0.18	0.06

#### 2.5. Contact model formulation

Concerning to the tool/chip and the tool/workpiece contacts, they can be represented by the model proposed by Zorev [14] for the shear stress  $\tau$ , with the friction coefficient  $\mu$  given by Eq. 12.  $\tau$  is expressed as follows:

$$\tau = \begin{cases} \mu \sigma_n & \text{if } \tau < \tau_{limite} \\ \tau_{limite} & \text{if } \tau > \tau_{limite} \end{cases} \quad (10)$$

$$\tau_{limite} = \frac{\sigma_y}{\sqrt{3}} \quad (11)$$

where  $\sigma_n$  is the normal stress,  $\tau_{limite}$  is the limit shear stress, and  $\sigma_y$  is the yield stress of the chip, calculated as described by Denguir et al. in [15].

The friction tests data permitted to identify an equation representing the adhesive friction coefficient in function of sliding velocity at the WC/OFHC copper interface. It is worth to notice that the shape of the friction coefficient evolution versus the sliding velocity is similar to that one found by Zorev [14], which can be approximated by the following equation:

$$\mu_{adh} = c_1 + \frac{c_2}{1 + [(v_s - c_3)/c_4]^2} \quad (12)$$

where  $c_i$  ( $i=1...4$ ) coefficients are 0.05, 0.323, 0.875 and 0.326, respectively.

The variation of the adhesive friction coefficient is shown in Fig. 4. The proposed friction model is valid for both applied normal forces of 200 N (Fig. 4a) and 500 N (Fig.

4b). The observed differences in the measured values concern mainly to the apparent friction coefficient at low sliding velocities, where the elasto-plastic deformation prevails. In literature, it is found that the friction coefficient generally decreases with the sliding velocity [16]. The variation of the friction coefficient with the sliding velocity having a maximum value for intermediate velocities is frequently observed for several materials [14]. The opposite case also exists, where the friction coefficient is minimal for intermediate sliding velocities [17].

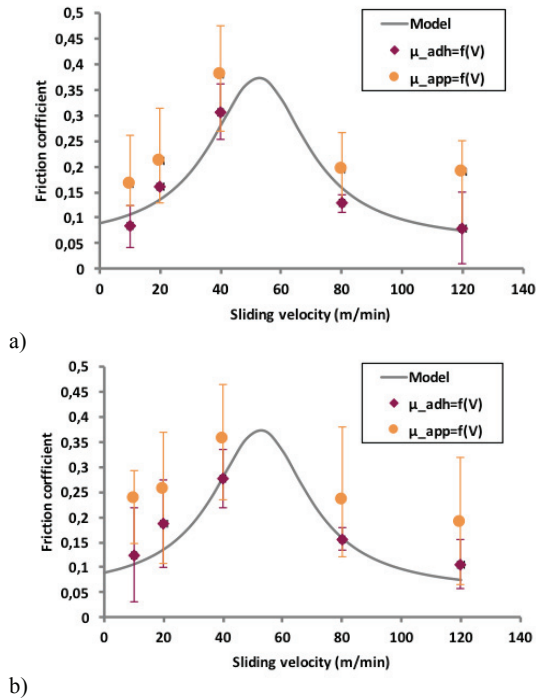


Fig. 4. Friction coefficients in function of the sliding velocity: experimental adhesive friction coefficient ( $\mu_{adh}$ ), apparent friction coefficient ( $\mu_{app}$ ), modeled adhesive friction coefficient (Model) at (a)  $F_n = 200$  N; (b)  $F_n = 500$  N.

### 3. Application of the friction model to orthogonal cutting simulation

#### 3.1. Numerical simulation of orthogonal cutting of OFHC copper using a tungsten carbide tool

A model is developed and applied to simulate the surface integrity induced by orthogonal cutting of OFHC copper, using the Arbitrary Lagrangian–Eulerian (ALE) formulation. A coupled temperature displacement analysis is performed using the FEA software ABAQUS/Explicit. Fig. 5 shows the model’s boundary conditions.

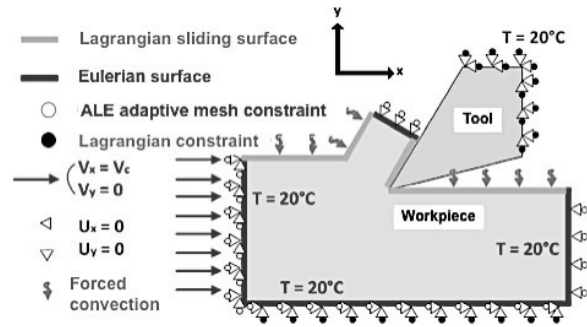


Fig. 5. Boundary conditions used in the simulation.

To model the mechanical behavior of OFHC copper and to predict the dislocations density, a user subroutine VUMAT is developed, integrating the material constitutive model taken from [15]. The elastic and thermal properties of the work material are also taken from [15]. The tool is modelled as elastic and its thermal and elastic properties are obtained from literature [18].

As already mentioned, the tool-chip and the tool-workpiece contacts were modelled by the Zorev’s model, using a friction coefficient in function of the sliding speed given by Eq. 10. For comparison purposes, an additional simulation using a constant friction coefficient of 0.3 was performed.

To calculate residual stresses, the workpiece is mechanically unloaded ( $V_c = 0$  m/min), and its temperature should reach the ambient temperature. To reach stresses equilibrium in the shortest time, implicit formulation is used. Therefore, the workpiece is transferred to ABAQUS™/Standard, including the field variables and the mechanical behavior of the material.

#### 3.2. Experimental setup for orthogonal cutting

Orthogonal cutting tests over flat specimens of 40(L)x15(H)x4(W) mm in OFHC copper (annealed, average grain size of 50  $\mu$ m and average hardness of 46 HB) were performed using planing configuration. These tests were performed on a DMG DMC85V milling machine. The cutting tool was uncoated cemented tungsten carbide with an edge radius ( $r_n$ ) of 10 $\pm$ 2  $\mu$ m, a clearance angle ( $\alpha$ ) of 10° and a rake angle ( $\gamma$ ) of 20°. The cutting speed ( $V_c$ ), uncut chip thickness ( $h$ ) and width of cut ( $a_p$ ) were kept constant and equal to 120 m/min, 0.2 mm and 4 mm ( $a_p = W$ ), respectively. Low temperature pressured air (-5 $\pm$ 2 °C, 6 bar) was applied to minimize the adhesion phenomenon between the tool and the work material.

#### 3.3. Setup for residual stress analysis

Residual stresses were analyzed by X-ray diffraction technique, using the  $\sin^2\psi$  method. According to this method, the residual stresses are calculated from strain distribution  $\epsilon_{\phi\psi\{hkl\}}$  derived from the measured inter reticular plane spacing and knowing the elastic radio crystallographic constants,  $S_{1\{hkl\}}$  and  $\frac{1}{2}S_{2\{hkl\}}$ , which are

equal to  $-3.13 \times 10^6 \text{ MPa}^{-1}$  and  $11.7 \times 10^6 \text{ MPa}$  for OFHC copper, respectively. An X-ray *Mn-K $\alpha$*  radiation is used to determine the elastic strains in the (311) planes (149,09° Bragg angle). The residual stresses are determined in the machined surface and subsurface, in the cutting and transversal directions. To determine the in-depth residual stress profiles, successive layers of material are removed by electro polishing, to avoid the reintroduction of residual stress.

3.4. Cutting simulations results and discussion

3.4.1. Influence of the friction coefficient on CCR

Chip Compression Ratio (CCR) is defined by the ratio between the chip thickness ( $h_1$ ) and the uncut chip thickness ( $h$ ). To evaluate the influence of using a friction coefficient depending on the sliding velocity in the predicted results, the CCR obtained by the proposed friction model is compared with the one obtained by a constant friction coefficient, and the experimental CCR value. The experimental measurement is performed on a numerical image captured by a rapid camera with a pulsed laser during the cutting process (Fig. 6).

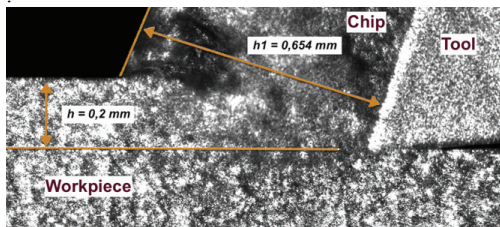


Fig. 6. Image of chip formation using LaVision Imager sCMOS double frame camera together with a Litron NS30-15 double-cavity pulsed laser at the tested cutting conditions.

As shown in Fig. 7, a variable friction coefficient in function of the sliding speed enhances the predicted CCR by reducing the difference between measured and predicted CCR from 0.72 (using constant friction) to 0.4 (using variable friction) (from 22% to 12%).

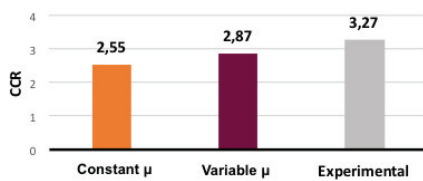


Fig. 7. Chip Compression Ratio (CCR).

3.5. Influence of the friction coefficient on temperatures

Besides the chip morphology, the friction model has shown an influence on the temperatures distribution in the chip and tool. As shown in Fig. 8, the tool/chip contact temperatures are lower when the friction coefficient is function of the sliding velocity.

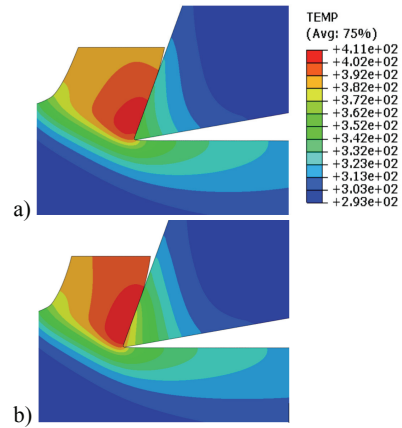
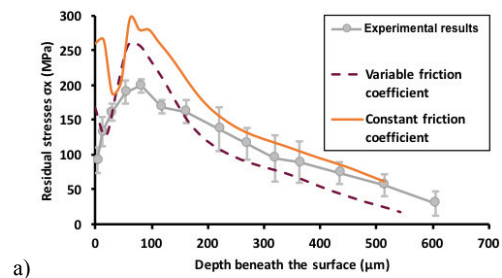


Fig. 8. Temperatures distributions in °K using (a) variable friction coefficient in function of the sliding speed, and (b) a constant friction coefficient.

3.6. Influence of the friction coefficient on residual stresses prediction

As orthogonal cutting model was developed for surface integrity prediction purposes, the influence of the friction model on the generated residual stresses in the machined surface and subsurface was evaluated. They are predicted and measured in the cutting direction ( $\sigma_x$ ), and in the direction parallel to the cutting edge ( $\sigma_y$ ).

As shown in Fig. 9, the use of a variable friction coefficient in function of the sliding speed demonstrates a slight difference in the in-depth residual stresses predictions, especially an improvement in the predicted values near the machined surface, and at the subsurface. These differences seen in the predicted residual stresses can be due to the influence of local sliding velocity on the material flow on the tool/work material interface. So, it alters the mechanical loading in the deformation zone during cutting. In fact, an overestimation of the friction coefficient induces an increase in the simulated forces, and consequently an increase in the deformation near the contact, including the flank zone (large tool–chip contact length and to a large stagnation zone around the cutting edge). For that reason, in the case where the friction coefficient is considered as a constant, the overestimation of the loading at the flank zone has induced an increase in the residual stresses.



a)

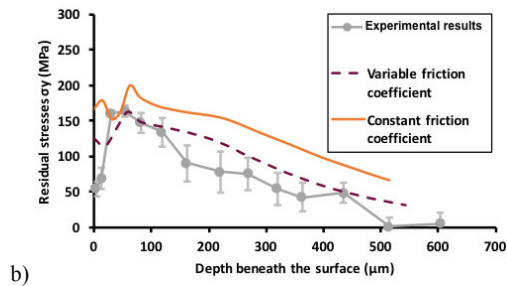


Fig. 9. Measured and predicted in-depth residual stresses profiles obtained using variable and constant friction coefficients.

#### 4. Conclusion and outlook

This work proposes a new friction coefficient model for tungsten carbide/OFHC copper contact, used to predict the residual stress and *CCR* in orthogonal cutting. This model was derived from pin on cylinder friction tests, performed using different sliding velocities and two contact pressures under forced cooled air conditions.

Orthogonal cutting simulations put in evidence some improvements in the predicted *CCR* and residual stress while a variable friction coefficient (function of the sliding speed) is used instead of a constant one. Nevertheless, this friction model should be improved by considering larger contact pressures.

#### Acknowledgements

The authors would thank CEA Valduc for the financial support. They would also acknowledge the LTDS - ENI St Etienne for the technical support in friction tests performance.

#### References

- [1] I. S. Jawahir, E. Brinksmeier, R. M'Saoubi, D. K. Aspinwall, J. C. Outeiro, D. Meyer, D. Umbrello, and A. D. Jayal, "Surface integrity in material removal processes: Recent advances," *CIRP Ann. - Manuf. Technol.*, vol. 60, no. 2, pp. 603–626, 2011.
- [2] S. Bissey-Breton, V. Vignal, F. Herbst, and J. B. Coudert, "ScienceDirect Influence of machining on the microstructure, mechanical properties and corrosion behaviour of a low carbon martensitic stainless steel," *Procedia CIRP*, vol. 46, no. 46, pp. 331–335, 2016.
- [3] V. P. Astakhov, *Tribology of metal cutting*. Elsevier, 2006.
- [4] O. Klinkova, J. Rech, S. Drapier, and J. M. Bergheau, "Characterization of friction properties at the workmaterial/cutting tool interface during the machining of randomly structured carbon fibers reinforced polymer with carbide tools under dry conditions," *Tribol. Int.*, vol. 44, no. 12, pp. 2050–2058, 2011.
- [5] S.-P. Lo Zone-Chin Lin, "Ultra-precision orthogonal cutting simulation for oxygen-free high-conductivity copper," *Mater. Process. Technol.*, vol. 65, pp. 281–291, 1997.
- [6] F. Ambrosy, F. Zanger, and V. Schulze, "FEM-simulation of machining induced nanocrystalline surface layers in steel surfaces prepared for tribological applications," *CIRP Ann. - Manuf. Technol.*, vol. 64, pp. 69–72, 2015.
- [7] R. Liu, M. Salahshoor, S. N. Melkote, and T. Marusich, "A unified material model including dislocation drag and its application to simulation of orthogonal cutting of OFHC Copper," *J. Mater. Process. Technol.*, vol. 216, pp. 328–338, 2015.
- [8] J. T. Carroll and J. S. Strenkowski, "Finite element models of orthogonal cutting with application to single point diamond turning," *Int. J. Mech. Sci.*, vol. 30, no. 12, pp. 899–920, 1988.
- [9] Y. Abushawashi, X. Xiao, and V. P. Astakhov, "FEM simulation of metal cutting using a new approach to model chip formation," *Int. J. Adv. Mach. Form. Oper.*, vol. 3, no. 2, pp. 71–92, 2011.
- [10] T. Moriwaki, "Machinability of Copper in Ultra-Precision Micro Diamond Cutting," *CIRP Ann. - Manuf. Technol.*, vol. 38, no. 1, pp. 115–118, 1989.
- [11] L. A. Denguir, J. C. Outeiro, G. Fromentin, V. Vignal, and R. Besnard, "Orthogonal Cutting Simulation of OFHC Copper Using a New Constitutive Model Considering the State of Stress and the Microstructure Effects," in *Procedia CIRP*, 2016, vol. 46.
- [12] Y. Zhang, T. Mabrouki, D. Nelias, C. Courbon, J. Rech, and Y. Gong, "Cutting simulation capabilities based on crystal plasticity theory and discrete cohesive elements," *J. Mater. Process. Technol.*, vol. 212, no. 4, pp. 936–953, 2012.
- [13] C. Courbon, V. Sajin, D. Kramar, J. Rech, F. Kosel, and J. Kopac, "Investigation of machining performance in high pressure jet assisted turning of Inconel 718: A numerical model," *J. Mater. Process. Technol.*, vol. 211, no. 11, pp. 1834–1851, 2011.
- [14] N. N. Zorev and M. C. Shaw, *Metal cutting mechanics. (Voprosy mekhaniki protsesssa rezaniia metallov)*. Pergamon Press, 1966.
- [15] L. A. Denguir, J. C. Outeiro, G. Fromentin, V. Vignal, and R. Besnard, "Orthogonal Cutting Simulation of OFHC Copper Using a New Constitutive Model Considering the State of Stress and the Microstructure Effects," *Procedia CIRP*, vol. 46, pp. 238–241, 2016.
- [16] C. Bonnet, F. Valiorgue, J. Rech, C. Claudin, H. Hamdi, J. M. Bergheau, and P. Gilles, "Identification of a friction model—Application to the context of dry cutting of an AISI 316L austenitic stainless steel with a TiN coated carbide tool," 2008.
- [17] V. P. Astakhov, "The assessment of cutting tool wear," *Int. J. Mach. Tools Manuf.*, vol. 44, pp. 637–647, 2004.
- [18] J. C. Outeiro, A. M. Dias, and I. S. Jawahir, "On the effects of residual stresses induced by coated and uncoated cutting tools with finite edge radii in turning operations," *CIRP Ann. - Manuf. Technol.*, vol. 55, no. 1, pp. 111–116, 2006.